View metadata, citation and similar papers at core.ac.uk
brought to you by CORE
provided by CLoK

Mon. Not. R. Astron. Soc. **414,** 2195–2203 (2011) doi:10.1111/j.1365-2966.2011.18536.x

A pre-outburst signal in the long-term optical light curve of the recurrent nova RS Ophiuchi

S. Adamakis,[1,2] S. P. S. Eyres,[1⋆] A. Sarkar[1,3] and R. W. Walsh[1]

[1]*Jeremiah Horrocks Institute, University of Central Lancashire, Preston PR1 2HE*
[2]*Decision Science, Lloyds Banking Group, 155 Bishopsgate, London EC2M 3TQ*
[3]*Space Science Centre, University of New Hampshire, Durham NH 03824*

Accepted 2011 February 13. Received 2011 February 13; in original form 2010 June 25

ABSTRACT

Recurrent novae are binary stars in which a white dwarf accretes matter from a less evolved companion, either a red giant or a main-sequence star. They have dramatic optical brightenings of around 5–6 mag in *V* in less than a day, several times a century. These occur at variable and unpredictable intervals, and are followed by an optical decline over several weeks and activity from the X-ray to the radio. The unpredictability of recurrent novae and related stellar types can hamper systematic study of their outbursts. Here we analyse the long-term light curve of RS Ophiuchi, a recurrent nova with six confirmed outbursts, most recently in 2006 February. We confirm the previously suspected 1945 outburst, largely obscured in a seasonal gap. We also find a signal via wavelet analysis that can be used to predict an incipient outburst up to a few hundred days before hand. This has never before been possible. In addition, this may suggest that the preferred thermonuclear runaway mechanism for the outbursts will have to be modified, as no pre-outburst signal is anticipated in that case. If our result indeed points to gaps in our understanding of how outbursts are driven, we will need to study such objects carefully to determine if the white dwarf is growing in mass, an essential factor if these systems are to become Type Ia supernovae. Determining the likelihood of recurrent novae being an important source population will have implications for stellar and galaxy evolution.

Key words: stars: individual: RS Oph – novae, cataclysmic variables.

1 INTRODUCTION

The binary star RS Ophiuchi (RS Oph) consists of a white dwarf (WD) orbiting within the dense wind of a red giant (RG). As the WD travels in its orbit it accretes matter from the RG wind, growing slowly in mass. The orbital period is around 460 d (Dobrzycka & Kenyon 1994), but the system does not eclipse as the inclination angle is approximately 50° to the line of sight, assuming a massive WD around 1.2–1.4 $M_{\odot}$ (Brandi 2009). It has experienced at least six dramatic optical brightening events or outbursts (in 1898, 1933, 1958, 1967, 1985 and 2006) generally attributed thermonuclear runaway (TNR) events within the accreted matter on the WD surface. Two other events are suggested in the literature (1907 and 1945 from Schaefer 2004 and Oppenheimer & Mattei 1993, respectively). The optical development during an outburst is very similar in each case (Rosino 1986). Following the 2006 outburst, a WD mass of around 1.35 $M_{\odot}$ has been suggested (Sokoloski et al. 2006) implying that RS Oph may be a Type Ia supernova progenitor.

Since the WD is gaining mass through accretion, but losing mass due to the outbursts, an interesting question is what happens to the overall mass of the WD after an outburst? Will it increase, stay unchanged or decrease over many outbursts? If it actually increases in mass, then this means that at some point it will exceed the Chandrasekhar limit, which will lead to a Type Ia supernova (Sokoloski et al. 2006). Supernovae outbursts play an important role in the history of the Universe and as standard candles. Being able to observe a complete recurrent nova cycle from pre-outburst accretion to post-outburst quiescence in sufficient detail will tell us a lot about the physical processes involved. If we were able to predict an outburst, we would be able to take spectroscopic and multiband observations of the star before and at the beginning of the outburst, which has never been done before.

Here we examine the optical light curve between 1933 and 2008, which includes five confirmed and one suspected outburst. The data have been taken from the American Association of Variable Star Observers (AAVSO; A. A. Henden, private communication) and are mainly visual estimates. In Section 2, we present the light curve over 75 yr and discuss previous work to analyse the variations. In Section 3, we look at a Bayesian approach to parametrizing the form of the light curve during the outbursts, describing the

⋆E-mail: spseyres@uclan.ac.uk

© 2011 The Authors
Monthly Notices of the Royal Astronomical Society © 2011 RAS

stages of post-outburst development and providing a model that supports the subsequent analysis of the whole light curve. Section 4 presents a wavelet analysis of the light curve, which leads to a pre-outburst signal that is present in the data even if we remove the outbursts themselves. In Section 5, we discuss this feature and its potential utility in predicting outbursts sufficiently early to allow detailed observations of the pre-outburst and peak periods of the next outburst.

2 OPTICAL LIGHT CURVE

Fig. 1 shows the AAVSO visual light curve from 1933 August 16 to 2008 January 31 (44 655 points over 27 196 d). These are mainly naked eye visual estimates from amateur astronomers, while more recently these are supplemented by *V*-band telescope measurements, also from amateur observers. There is considerable scatter, but the data is of sufficient quality to determine some basic features.

(i) There are clear peaks in 1933, 1958, 1967, 1985 and 2006 due to the optical brightening – this is the fundamental activity that identifies an object as a recurrent nova.

(ii) The quiescent light curve fluctuates between 9.6 and 12.8 mag, but with no periodicity or other pattern.

(iii) The time from outburst to decline to quiescent mean magnitude is about 100 d, but the light consistently declines below this point and only recovers to approximately the mean after 400–500 d.

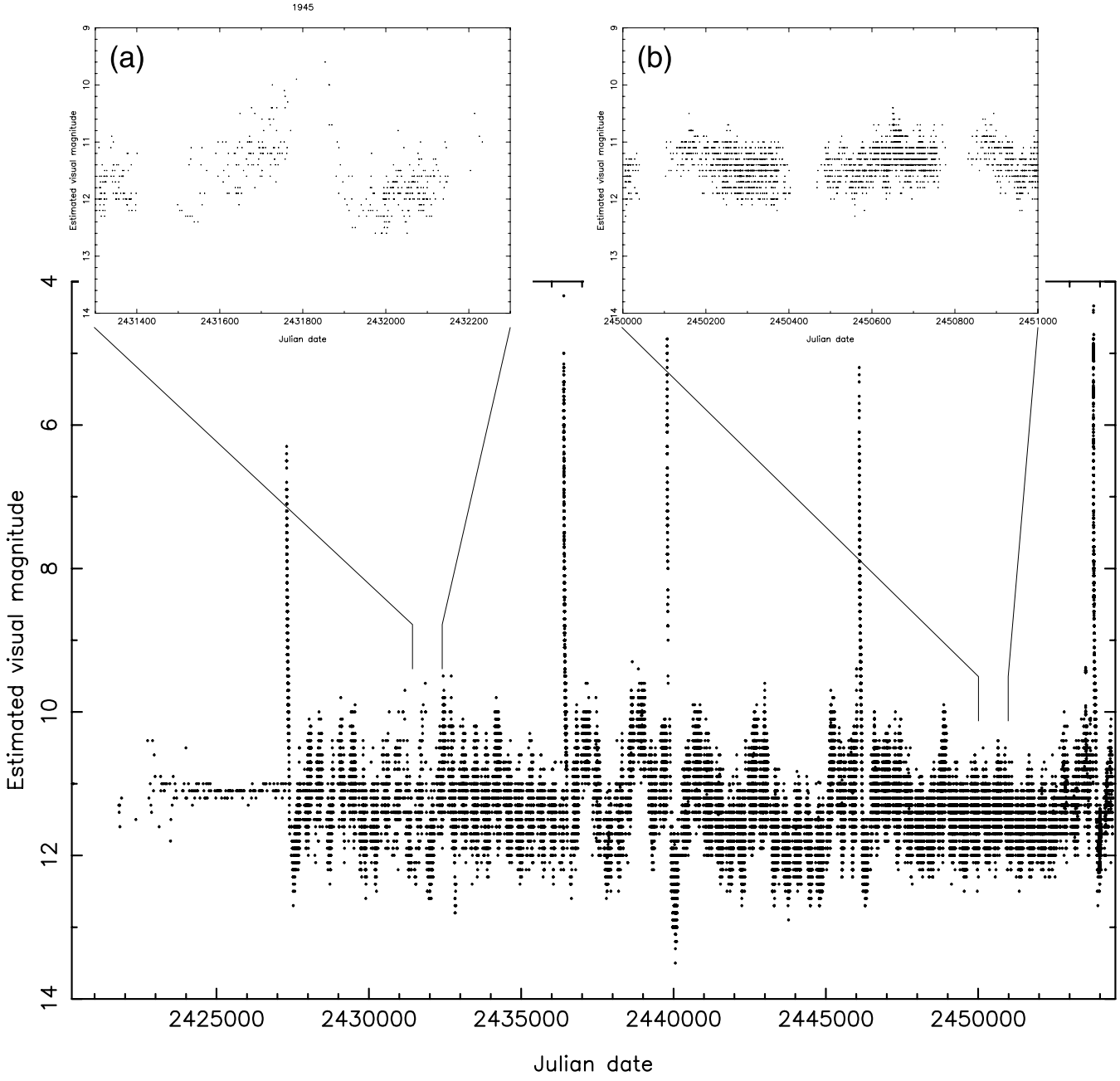

Figure 1. Optical light curves from 1933 to 2008, mainly visual estimates from the AAVSO. Panel (a) shows the 1000 d centred on 1945 (see Fig. 2), while panel (b) shows the 1000 d centred on 1997, showing a typical quiescent period including two seasonal gaps. The horizontal 'stripes' are due to the data being recorded to only the nearest 0.1 mag on the AAVSO database.

(iv) The seasonal gap from mid-November to January is long enough to contain most of an outburst, so we may have missed one or more. However, each decline-and-recovery phase is sufficiently similar and lasts long enough that the tail of such a hidden outburst might be identifiable.

As we examine the characteristics of the outbursts, we also present the 1000 d around each outburst in Fig. 2. We also include the data around 1945 that led Oppenheimer & Mattei (1993) to suggest an outburst that was missed in the seasonal gap.

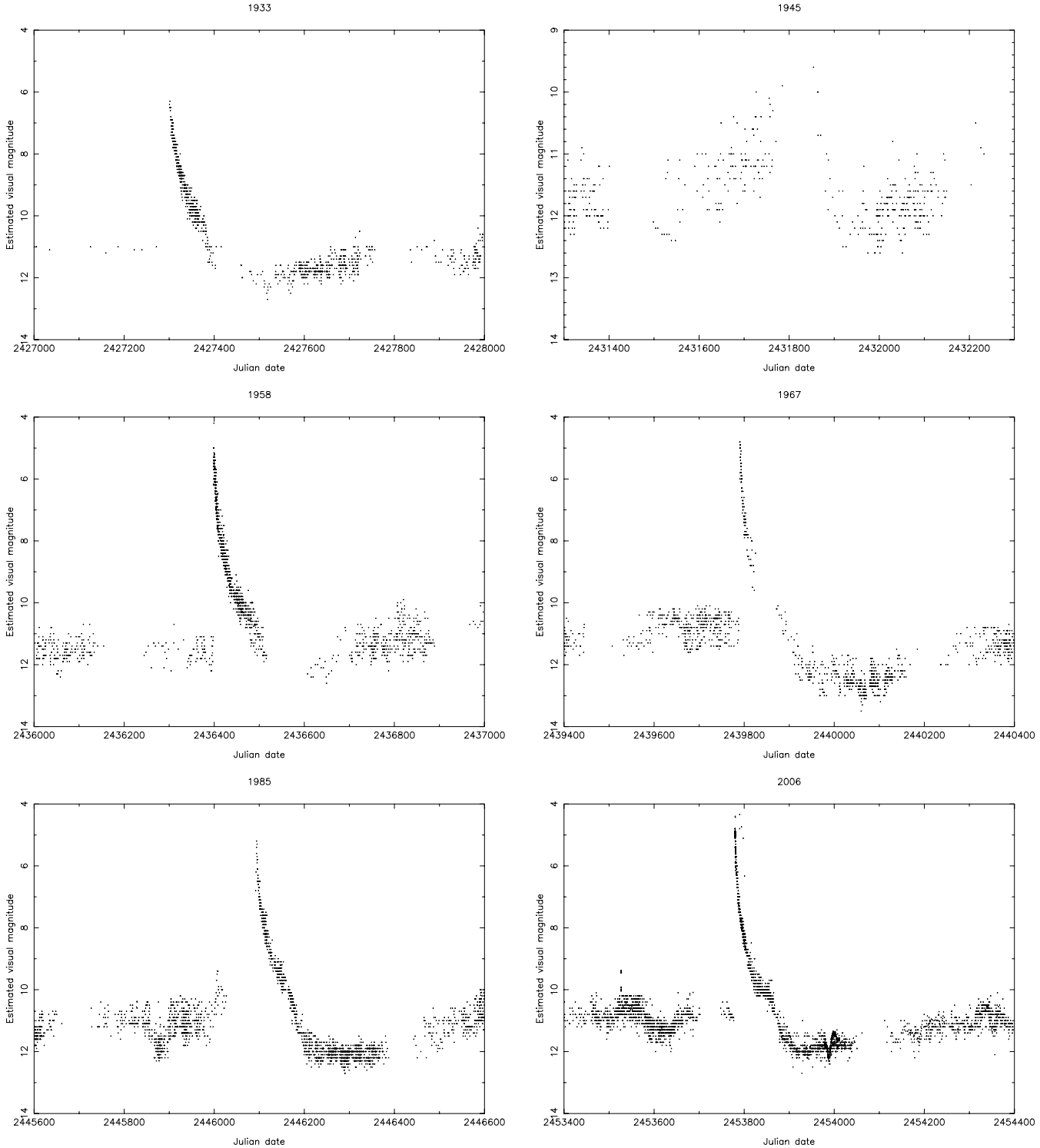

Figure 2. Five confirmed outbursts present in Fig. 1 in the years as marked, plus the period of time in 1945 that Oppenheimer & Mattei (1993) propose shows the final decline and recovery phases of the sixth outburst. This panel is on a different vertical scale and is also presented in Fig. 1 panel (a) to enable a comparison with a typical quiescent period in Fig. 1 panel (b). Also apparent in these panels is the increase density of data with time over the 75 yr presented.

© 2011 The Authors, MNRAS **414,** 2195–2203
Monthly Notices of the Royal Astronomical Society © 2011 RAS

A number of authors (Dobrzycka, Kenyon & Milone 1996; Sokoloski, Bildsten & Ho 2001; Gromadzki et al. 2006; Worters et al. 2007; Zamanov et al. 2010) have found flickering-like fluctuations on time-scales of minutes, and Worters et al. (2007) were the first to detect the resumption of flickering post-outburst. As flickering of this sort is generally attributed to accretion in binary star systems, this enabled the first post-outburst accretion rate estimate to be made. The AAVSO light curve presented here has insufficient time resolution to allow flickering analysis. However, it should be noted that night-to-night variations of 0.5 mag are seen in high time resolution data, so that the AAVSO data have some sensitivity to the underlying amplitude of flickering.

We extract the outburst events from Fig. 1 and conduct a Bayesian analysis to characterize the decline described in Section 3. We also use the data in Fig. 1 as the basis of a wavelet analysis with a Morlet mother function (Torrence & Compo 1998), as described in Section 4.

3 DECLINE OF THE LIGHT CURVE FOLLOWING AN OUTBURST

Oppenheimer & Mattei (1993) discussed the decline rate of the outbursts. They divided each outburst into different phases according to the decline rate and concluded that each outburst consists of three break points before the star begins to brighten again. In this section, we model the outburst data with simple curves. The aim is simply to parametrize the form of the decline, rather than determine any underlying physical model.

In order to apply the statistical analysis, we take the first 500 d of each outburst (including the proposed 1945 one). The total number of data values is $n = 8505$. The most well-observed outburst is the one that happened in 2006 with 4109 observed points. The more observed points there are in an outburst, the more information will be added from this outburst to the statistical analysis we undertake. Oppenheimer & Mattei (1993) commented that the decline rate and then brightening rate of the proposed 1945 (obscured) outburst is akin to all the other outbursts and that this combination has never been observed outside of an outburst. From this resemblance of the light curves, we have a reason to believe that the same physical mechanisms cause all the outbursts. Hence, we can assume that all the outbursts can be described with the same parametrized model.

3.1 Models for Bayesian analysis

We apply Bayesian analysis to the declines from maximum for each outburst in the data. We consider four models. In each case, the time $t_4 = 500$ d defines the end of the outburst, and the parameters $\gamma_1, \gamma_2, \gamma_3$ and γ_4 are calculated to ensure each model is continuous. We take time zero as a parameter to determine the start of each outburst, instead of assuming it is defined by the first observed point in outburst; this allows us to estimate the start date of the proposed 1945 outburst and hence check that it would not have been visible before the seasonal gap. The break points in the decline are calculated as times t_1, t_2 and t_3 from this zero-point.

Model 1. This is the most complicated model of the four with 11 free parameters. It consists of four stages. During the first three stages, there is a decline in magnitude, whereas in the last one it increases:

$$M_1 : \mu = \begin{cases} \gamma_1 + \alpha_1 \log(t + \beta_1), & 0 \le t < t_1 \\ \gamma_2 + \alpha_2 \exp(\beta_2 t), & t_1 \le t < t_2 \\ \gamma_3 + \alpha_3 \exp(\beta_3 t), & t_2 \le t < t_3 \\ \gamma_4 + \alpha_4 t, & t_3 \le t < t_4 \end{cases} . \quad (1)$$

The parameter space for this model will be $P_1 = (\gamma_1, \alpha_1, \beta_1, t_1, \alpha_2, \beta_2, t_2, \alpha_3, \beta_3, t_3, \alpha_4)$.

Model 2. This is the second most complex model with 10 free parameters. It consists of four stages. The only difference between this and the M_1 model is the third stage, where instead of an exponential function we assume a straight line:

$$M_2 : \mu = \begin{cases} \gamma_1 + \alpha_1 \log(t + \beta_1), & 0 \le t < t_1 \\ \gamma_2 + \alpha_2 \exp(\beta_2 t), & t_1 \le t < t_2 \\ \gamma_3 + \alpha_3 t, & t_2 \le t < t_3 \\ \gamma_4 + \alpha_4 t, & t_3 \le t < t_4 \end{cases} . \quad (2)$$

The parameter space for this model will be $P_1 = (\gamma_1, \alpha_1, \beta_1, t_1, \alpha_2, \beta_2, t_2, \alpha_3, t_3, \alpha_4)$.

Model 3. This model consists of nine free parameters and four stages. The only change from the M_2 model is the second stage, where instead of an exponential function we assume a straight line:

$$M_3 : \mu = \begin{cases} \gamma_1 + \alpha_1 \log(t + \beta_1), & 0 \le t < t_1 \\ \gamma_2 + \alpha_2 t, & t_1 \le t < t_2 \\ \gamma_3 + \alpha_3 t, & t_2 \le t < t_3 \\ \gamma_4 + \alpha_4 t, & t_3 \le t < t_4 \end{cases} . \quad (3)$$

The parameter space for this model will be $P_1 = (\gamma_1, \alpha_1, \beta_1, t_1, \alpha_2, t_2, \alpha_3, t_3, \alpha_4)$.

Model 4. This is the simplest model with seven free parameters. The basic difference between this and the previous three models is that it consists of three stages. In the first two the stages, the magnitude is declining and in the third it is increasing:

$$M_4 : \mu = \begin{cases} \gamma_1 + \alpha_1 \log(t + \beta_1), & 0 \le t < t_1 \\ \gamma_2 + \alpha_2 t, & t_1 \le t < t_2 \\ \gamma_3 + \alpha_3 t, & t_2 \le t < t_3 \end{cases} . \quad (4)$$

The parameter space for this model will be $P_1 = (\gamma_1, \alpha_1, \beta_1, t_1, \alpha_2, t_2, \alpha_3)$.

In the following analysis, we assume that the first observed brightest point of each outburst is at time $\tau_j, \quad j = 1, \ldots, 6$ from the true beginning of the outburst (there are six outbursts including the 1945 one). We incorporate $P_2 = (\tau_1, \ldots, \tau_6)$ as parameters so that the data will decide their values. This will also give us the information about how many days after the 1945 peak the first observation occurred. Therefore, the parameter space will be $P = (P_1, P_2)$.

Uninformative prior distributions were assumed for the parameters, where possible. Also normal and uncorrelated errors were implemented for the observed values. In this case, nuisance parameters like the standard deviation of the errors can be integrated out.

3.2 Preferred model

First, we will try to choose which of the four models fits best to the data we have, and after that we present the parameter estimations for that particular model. The codes used for this analysis were written and implemented by Adamakis (2009).

Table 1 depicts the logarithmic marginal densities estimation with three different approximation methods. All of them choose model M_2 as the best, although M_2 is 'not more than a bare mention' better than M_3, according to the criteria of Kass & Raftery (1995). The information criteria (Table 2) choose M_2 and M_3 as the best two models. However, they disagree as Akaike Information Criterion (AIC, Akaike 1974) suggests M_2, whereas Bayesian Information Criterion (BIC, Schwarz 1978) proposes M_3. The maximum likelihood functions under these two models are $-26\,235.67$ for M_2

Table 1. Logarithmic marginal densities estimation for modelling RS Oph's outbursts.

	M_1	M_2	M_3	M_4
1	−26 276.07	−26 271.55	−26 272.58	−26 301.42
2	−26 277.63	−26 272.27	−26 273.36	−26 302.03
3	−26 279.96	−26 274.97	−26 275.29	−26 301.33

Notes. 1 – Laplace method with posterior covariance matrix; 2 – Laplace method with robust posterior covariance matrix; 3 – importance sampling estimation with the probability density from stage 1 as the additional probability density.

Table 2. Information criteria and maximized log-likelihood functions for the $M_j, j = 1, \ldots, 4$ models.

	M_1	M_2	M_3	M_4
AIC	52 505.30	52 503.35	52 504.38	52 568.91
BIC	52 625.12	52 616.12	52 610.11	52 660.54
Maximum log-likelihood	−26 235.65	−26 235.67	−26 237.19	−26 271.46

and −26 237.19 for M_3. Although M_2 maximizes the likelihood compared to M_3, the fact that it contains one more parameter than M_3 does not allow Bayes factor estimations to clearly favour M_2. Therefore, M_3 cannot be excluded. Nevertheless, we select model M_2 for further analysis.

Table 3 provides all the information we need for the parameter estimation. We will not comment separately on each parameter because there are too many. Instead, we will try to focus on the most important ones. Starting with the break point parameters, we can estimate t_1 to be ∼53 d from the actual beginning of the outburst (a 95 per cent probability credible interval will give it to be between ∼49 and ∼59 d). Between ∼53 and ∼107 d (95 per cent credible interval between 102 and 109) from the beginning of the outburst, the decline rate changes from logarithmic to exponential. The decline is completed ∼143 d after the beginning of the actual outburst (95 per cent credible interval between ∼139 and ∼146 d). The decline rates can be taken from parameters α_1, β_1, α_2, β_2, α_3 and α_4, with the α values in units of mag d^{-1}.

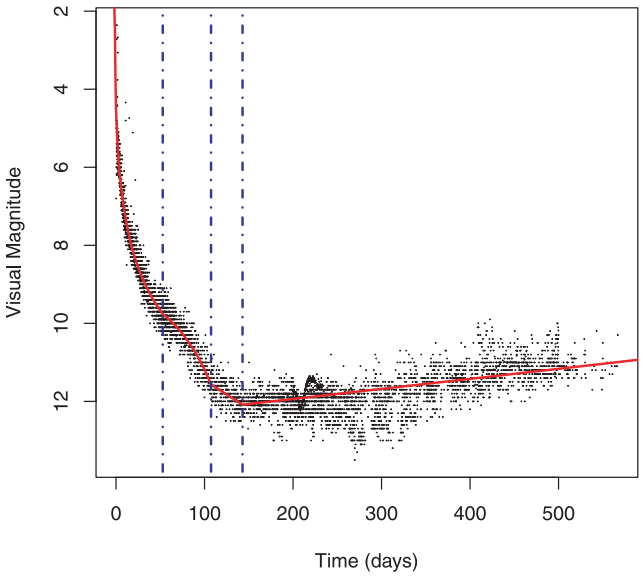

Figure 3. Compiled declines from every outburst in Fig. 2, (first observed point to 500 d after peak) including the proposed 1945 outburst, demonstrating the similarity of all outbursts. The red solid line indicates the best fit from the Bayesian analysis (M_2). Dot–dashed blue lines indicate the break points, also from the Bayesian analysis.

The first observed data point for the 1945 outburst was ∼68 d after the modelled beginning of the outburst. The fact that the seasonal gap started 69.20 d before the first observed point means that there was an outburst only a few days after we entered the seasonal gap. Especially for τ_2, a 95 per cent credible interval will give a value between 63.09 and 69.09 d. We were more lucky with the 1985 outburst because before the first observed data point, there was a seasonal gap of 65.40 d. Since the modal value for the start of the 1985 outburst $\widehat{\tau}_5 = 0.01$ d, it may be concluded that this outburst started just after the end of the seasonal gap. All the other outbursts did not seem to have any observational gaps before the first observed data points, giving us the chance to observe them almost at the beginning. Fig. 3 shows all the outburst data aligned by the start date. The red solid line depicts the chosen model (M_2),

Table 3. Summary of the posterior inference for the M_2 model. Parameter τ_2 is the start point of the 1945 outburst. All times are in days since the modelled start points.

	Mean	Mode	Standard deviation	2.5 per cent	50 per cent	97.5 per cent
γ_1	2.89	2.87	0.09	2.70	2.90	3.07
α_1	1.71	1.72	0.03	1.66	1.71	1.76
β_1	2.53	2.53	0.18	2.19	2.52	2.91
t_1	53.07	52.79	2.61	48.77	52.75	59.13
α_2	0.25	0.29	0.09	0.10	0.26	0.42
β_2	0.02	0.02	3.18×10^{-3}	1.80×10^{-2}	2.18×10^{-2}	3.01×10^{-2}
t_2	106.00	107.36	1.77	102.01	106.10	109.12
α_3	0.02	0.01	1.65×10^{-3}	1.22×10^{-2}	1.51×10^{-2}	1.87×10^{-2}
t_3	142.89	142.95	1.79	139.40	142.91	146.41
α_4	-2.55×10^{-3}	-2.57×10^{-3}	5.06×10^{-5}	-2.65×10^{-3}	-2.55×10^{-3}	-2.45×10^{-3}
τ_1	3.45	3.47	0.24	2.98	3.45	3.93
τ_2	67.01	67.97	1.63	63.09	67.32	69.09
τ_3	0.62	0.66	0.07	0.42	0.64	0.70
τ_4	0.38	0.41	0.15	0.08	0.38	0.67
τ_5	0.09	0.01	0.08	2.45×10^{-3}	0.06	0.29
τ_6	0.45	0.49	0.10	0.24	0.46	0.65

whereas the blue dashed lines show the break points as the modal values $\widehat{t}_1$, $\widehat{t}_2$ and $\widehat{t}_3$.

From this, we have demonstrated that the 1945 data are consistent with an outburst beginning and completing most of its decline during the seasonal gap, but with the final decline and recovery visible. It does not prove that this is an outburst, as we included it in our analysis. But it is the simplest explanation of the data. As noted by Oppenheimer & Mattei (1993), the data that are available show a form that is only seen after outbursts. If we accept that there was an outburst at this time, the mean recurrence interval goes down. Between 1933 and 1967 the mean interval was just over 10 yr, compared with a mean over all seven outbursts of approximately 15 yr.

4 WAVELET ANALYSIS

We have subjected the light curve in Fig. 1 to a wavelet analysis using the techniques of Torrence & Compo (1998). We applied the implementation of these techniques in the FORTRAN 77 software available from those authors available via atoc.colorado.edu/research/wavelets. In order to apply a wavelet analysis, the data must be evenly sampled. Thus, we have resampled to a 1-d interval. Where a day had more than one observation, we have taken an average, while we take a linear interpolation from the adjacent dates over days with no data. Seasonal gaps are replaced with the mean value for the entire light curve. As 90 per cent of the data are from the quiescent periods, the effect of outbursts on the mean is small. As the analysis relies on a range of input data to generate each point in the output data, we pad beyond the start and end of the data with the mean value, until the total number of data points reaches the next power of two. While we used a Morlet mother function (Torrence & Compo 1998) that is designed to identify periodic signals in the data, power appears in the resultant power plot due to discontinuities in the data such as those seen at outburst.

While a complex wavelet function, such as used here, can allow the separation of both phase and amplitude of the data and is useful for identifying oscillations, a real wavelet function merges these two in one component and can be helpful to isolate peaks or discontinuities (Meyers, Kelly & O'Brien 1993). In this paper, the wavelet power spectrum is defined as the sum of the squares of the real and imaginary parts of the wavelet transform (Torrence & Compo 1998). Formally, there is a cone of influence (COI), outside which there is not enough information to determine if a signal is real. Primarily this excludes periods longer than the time-span of the data, but early and late in the time series it is also affected by the padding, hence the cone-like shape. More specifically, the wavelet power is expected to drop as we approach the edge of the data, due to the infinite support of the Morlet wavelet function.

Fig. 4(a) depicts the wavelet power plot of the optical light curve in Fig. 1 following resampling to a 1-d interval and interpolation of missing data as described above. The vertical dotted lines represent the beginning of an outburst as determined from our parametrization approach. All the peaks in the wavelet power spectrum are associated with an outburst. A similar feature can be located for the year 1945, where Oppenheimer & Mattei (1993) suggested an additional outburst. However, the wavelet power is not as strong as all the other outbursts due to the lack of data during the brightest part of the outburst (as we found in Section 3 if an outburst had indeed occurred, it started during the seasonal gap).

The most prominent peak in the wavelet power spectrum of Fig. 4(a) is linked with the 1967 outburst. This has to do with the fact that during the last stage of the magnitude decline of the outburst the magnitude becomes fainter than 12, which might be an

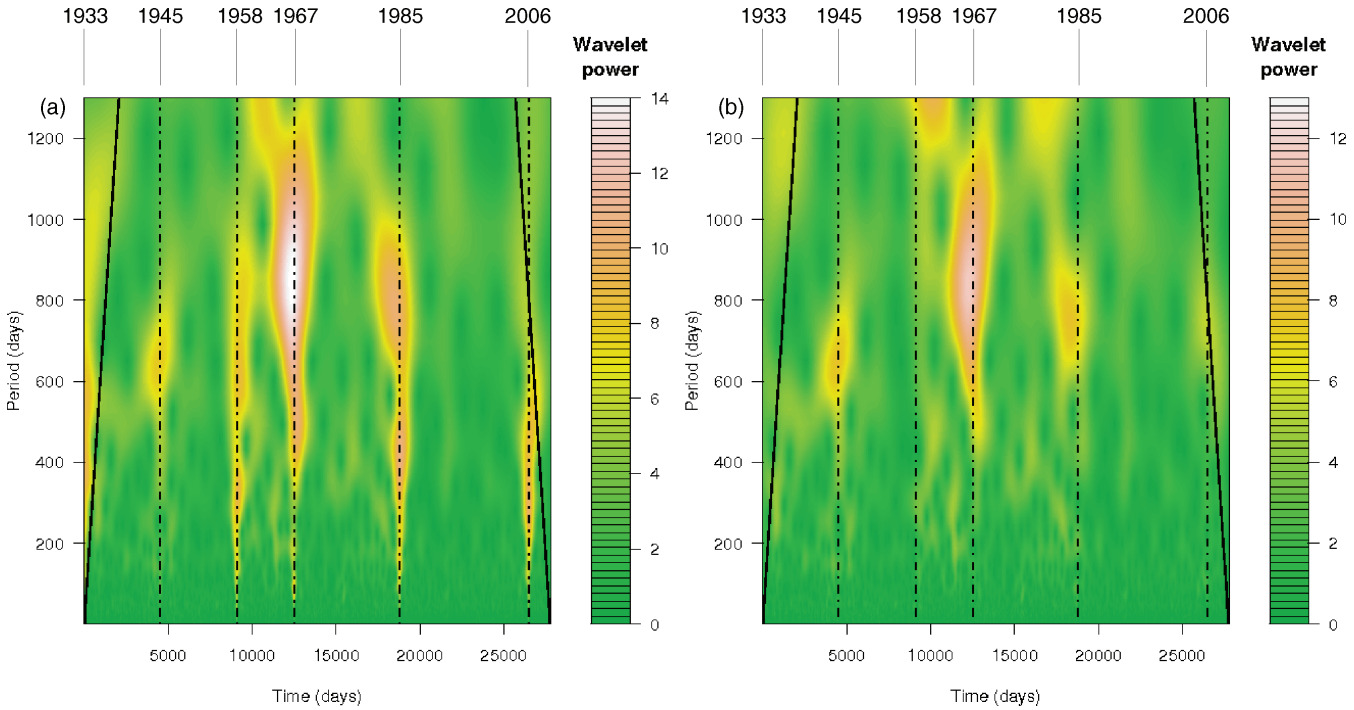

Figure 4. Wavelet power plot of the light curve in Fig. 1, panel (a) with the outbursts retained and panel (b) after replacing the outburst data with the mean of the data set. Outburst dates are marked. Note that the pre-outburst signal remains even in the absence of the outburst discontinuity and is visible for the 1945 obscured outburst. The scale of the power is different in panels (a) and (b), as indicated by the scale bars in each case.

indication that the 1967 outburst was more powerful than the others observed. Note that the features we observe are not symmetric about the beginning of each outburst. This asymmetry is because the wavelet power is influenced by the data before and after the outbursts. The signal for the 2006 outburst seems to be weaker than the rest of the outbursts because part of it is outside of the COI. This means that the wavelet power at larger scales will decrease as we approach the edges because we pad the end of the time series with the mean value.

4.1 Pre-outburst signal

A natural response of the wavelet power to discontinuities in the data (such as those seen at outburst in Fig. 4a) is a peak in the power at the time of the discontinuity. We decided to remove the first 143 d of each outburst and undertake the same analysis. The removed data have been replaced with the mean of the time series, as presented in Fig. 4(b). We tested the robustness of the results for different choices for replacement data, including a sinusoid of 50-d period and the residuals of subtracting the model determined in Section 3. Introducing different artificial values for the removed data did not affect the outcome of this analysis other than to insignificantly change the detailed distribution of power in the wavelet power spectrum.

Fig. 4(b) shows the resultant wavelet power spectrum. There are peaks in the wavelet power spectrum at a period range between 600 and 800 d that are associated with each of the 1945, 1985 and 2006 pre-outburst phases. This implies that these three outbursts are most similar regarding the light curve. The fact that part of the 2006 peak of the wavelet power is outside of the COI does not suggest that the wavelet power is completely wrong. Since we pad with the mean value of the time series at the edges, we expect the wavelet power near the edges at large scales to be less than it otherwise would be. This means that if we had more years of data, then the 2006 wavelet power peak would be entirely inside the COI and appear with enhanced wavelet power. The 1967 outburst is associated with a feature in the period range 500–1100 d, whereas the 1958 outburst does not give any significant peak associated with the pre-outburst. Thus we believe that the peak for 1958 in the wavelet power spectrum in Fig. 1(b), when the outburst data is retained, is due only to the data discontinuity. It is clear that all of the other outbursts (apart from the 1958 outburst) are linked with a specific form of wavelet power variation roughly around a period of 700–800 d which appears before the outburst begins, and so cannot be due to the discontinuity. Last but not least, the pre-outburst phase and the post-outburst phase (i.e. after 143 d from the outburst) of the light curve seem to follow the same pattern in all cases.

This is another indication why we should remove the outbursts from the analysis, as the peak for the wavelet power for the 1958 outburst in Fig. 4(a) is created only by the data discontinuity. Therefore, the 1958 and the 1967 outbursts might have progressed differently and may provide a key to the outburst mechanisms. In addition, the 1958 outburst was only 9 yr before the 1967 outburst, and also the 1958 outburst was not associated with any fluctuation around that range.

To conclude, each outburst is associated with a peak in the wavelet power spectrum around the 500–1000 d period (apart from the 1958 outburst), which never appears elsewhere in the lightcurve. A detailed analysis shows that these peaks are part of the true signal and not due to the observational uncertainty.

5 DISCUSSION

From our Bayesian analysis, using a piecewise model curve fitting for the declines from outburst, we find break points in the decline at ∼53, ∼107 and ∼143 d after the outburst. It is not clear that these are associated with any other changes in the system's behaviour. The X-ray flux shows a change in the power law of the decline at around day 70 (Bode et al. 2008; Ness et al. 2008), but there is no obvious physical reason to relate this to changes in the optical light curve. The supersoft phase also settled into a reasonably stable state around day 50 (Hachisu, Kato & Luna 2007), but again this cannot be clearly associated with the optical break by any physical mechanism.

It was found that the first observed point of the 1945 outburst was ∼68 d after the actual beginning of the outburst, which means that there was probably an outburst beginning at most a few days after the seasonal gap began. Using wavelet analysis, the pre-outburst and post-outburst features in the light curve at this time can be distinguished and are similar to all the other outbursts (apart from the 1958 one). Identifying an outburst in 1945 reduces the mean interval outburst recurrence rate from ∼20 yr (Starrfield 2006) to ∼12.5 yr. This also makes the 9-yr interval between the 1958 and 1967 outbursts less anomalous, moving it much closer to the median interval than when the 1945 outburst is excluded (from 1.25 to 0.7 standard deviations).

A more detailed look at the wavelet power for each outburst suggests that the 1945, 1985 and 2006 outbursts had similar magnitude wavelet peaks. The 1967 outburst has an unusually strong wavelet peak, while in the 1958 outburst there is no significant peak. While we can say nothing about the outburst mechanisms from this, it does suggest some observable pre-outburst activity in most cases – with the only analysed outburst without such a peak followed by a second outburst within 9 yr, still the shortest observed interval. The only major parameter in outburst models (e.g. Yaron et al. 2005) that can be varied on such short time-scales is the mass accretion rate on to the WD. Variable mass transfer also seems to be the only plausible process that could generate the pre-outburst activity indicated by our wavelet analysis. We note that the pre-outburst signal in the power plots are similar regardless of whether we include or exclude the outbursts themselves in the light curve (compare Figs 4a and b).

If we know what a typical characteristic of each outburst is, then we can use it for outburst prediction. Even 200 d before the outburst, the wavelet analysis shows this pre-outburst trend of the star. For 455 d before an outburst peak (an orbital period) this feature is less significant, but in some cases (the 1967 and 1985 outbursts) it is still recoverable. Hence, we have a means to predict outbursts in this object. Further work will extend this to similar systems. If it turns out to be robust, then it may also have implications for the outburst mechanism as a TNR should have no pre-outburst signal.

5.1 Outbursts prediction

Since (almost) every analysed outburst is linked with a pre-outburst feature in the wavelet power spectrum, this can be a useful tool for outburst prediction. To test this, wavelet analysis for the time interval between two outbursts has been applied. The starting point of each time series was 500 d after the beginning of the outburst. The end point of each time series was 455 d before the beginning of the next outburst, which coincides with one orbital period. The aim here was to investigate the appearance of the pre-outburst signal as we approach outburst.

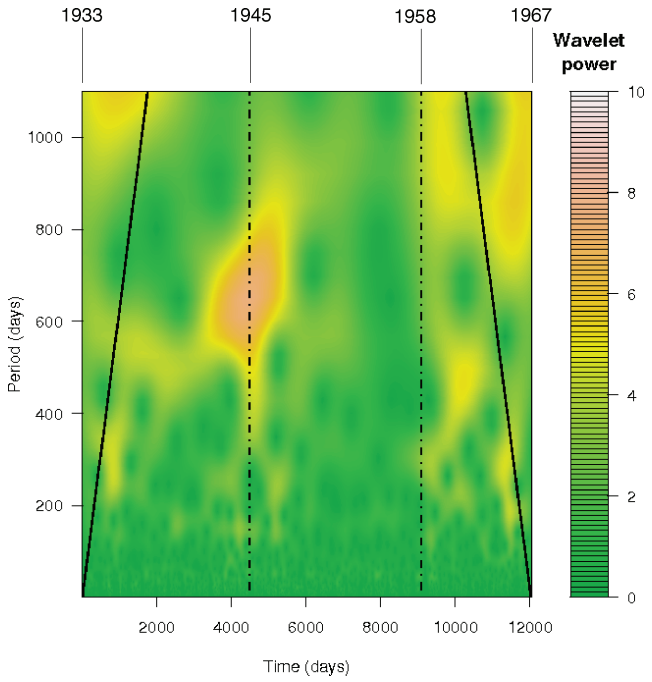

Figure 5. Wavelet power plot restricted to the time period between 1933 and 1967 showing the outburst feature for the 1945 outburst which was largely obscured by the seasonal gap.

In Fig. 5, data values between the 1933 and the 1967 outbursts were analysed. We can clearly see the peak in the wavelet power spectrum at a period around 600–800 d associated with the start of the 1945 outburst determined in Section 3. No such signal is apparent for the 1958 outburst, consistent with the result for the entire data set. The pre-outburst signal for the 1967 outburst is growing, albeit outside the COI. A similar analysis of the period from 1958 to 2006 showed similar signals for each outburst, with the 1967 one being by far the strongest.

The wavelet power of this peak drops as we approach the end of the time series because more wavelet function is convolved with the artificial data we padded the end of the time series with. The interaction of the true data with the artificial data will reduce the value of the wavelet power, the structure of which can only be influenced by changes in the real data. Although this feature is initially outside of the COI, it can still be recognized. As no other feature like this at that period range can be observed in the rest of the time series, this is consistent with the appearance of such a feature at the most recent end of the wavelet power plot indicating an approaching outburst. When we assumed we did not know that at the end of these data there was an outburst and did the same analysis up to (i) 1 d before the outburst, (ii) 100 d before the outburst and (iii) 200 d before the outburst, we still see this feature for every outburst where one was seen when the data from either side of the outburst were included (1945, 1967, 1985 and 2006). The closer we get to the outburst, the better defined this feature is. Similar analysis has been applied to all the time intervals between each pair of outbursts. The outcome was that a peak in the wavelet power spectrum like the one in Fig. 5 was observed before every outburst, apart from the 1958 outburst. Given that this also had the shortest interval to the next outburst in 1967 (which was then the strongest outburst seen so far), it may be that something peculiar happened at that date compared with the other outbursts. We do not have data before 1933 at sufficient density to subject to this analysis, so we cannot say anything about that outburst or the one in 1898.

6 CONCLUSION

We have analysed 76 yr of optical photometry of the recurrent nova RS Ophiuchi, allowing analysis of both the quiescent and outburst phases over that time. Bayesian analysis of the decline from maximum of the combined data from the five accepted outbursts in the data and the proposed 1945 outburst show that there is a preferred set of break points when the form of the decline changes, at ∼53, ∼107 and ∼143 d after the outburst peak, after which the optical light recovers towards the quiescent level over another ∼65 d. With this empirical model of the decline, we are able to place the start point of the 1945 outburst proposed by Oppenheimer & Mattei (1993) as only about a day after the start of the preceding seasonal gap. The 1945 data contribute so little to the Bayesian analysis that we can be confident that the decline seen here, but nowhere else in the light curve outside of a confirmed outburst, is due to the seventh outburst as proposed by Oppenheimer & Mattei (1993).

Turning to the overall light curve, including the quiescent phases, a wavelet analysis shows that there is a signal in wavelet power due to the outbursts. While some of this signal is contributed by the discontinuity due to the outburst, replacing the outburst data with continuous data essentially indistinguishable from quiescent data only reduces the strength of the signal prior to the known start dates for the outbursts. Thus it appears that we have identified a pre-outburst signature up to 450 d before the outburst in the wavelet analysis, which was apparent in all but the 1958 events. This holds out the possibility of having an early warning of outbursts in the future. It also suggests some implications for the accretion process at the onset of the outburst, as a TNR would not provide such a pre-outburst signal. We are working to extend this work to similar objects.

ACKNOWLEDGMENTS

We thank Dr. Mike Marsh for creating an independent plot equivalent to Fig. 4 as part of checking the outcomes for this paper. The wavelet analysis was applied using the wavelet software of Torrence and Compo (available at atoc.colorado.edu/research/wavelets). We acknowledge with thanks the variable star observations from the AAVSO International Database contributed by observers worldwide and used in this research. SA was supported by a PhD studentship from the University of Central Lancashire and the Science & Technology Facilities Council.

REFERENCES

Adamakis S., 2009, PhD thesis, Univ. Central Lancashire
Akaike H., 1973, in Petrov B. N., Csaki F., eds, 2nd International Symposium on Information Theory. Akademiai Kiado, Budapest, p. 267
Bode M. F. et al., 2008, in Evans A., Bode M. F., O'Brien T. J., Darnley M. J., eds, ASP Conf. Ser. Vol. 401, RS Ophiuchi (2006) and the Recurrent Nova Phenomenon. Astron. Soc. Pac., San Francisco, p. 269
Brandi E., Quiroga C., Mikotajewska J., Ferrer O. R., García L. G., 2009, A&A, 497, 815
Dobrzycka D., Kenyon S. J., 1994, AJ, 108, 2259
Dobrzycka D., Kenyon S. J., Milone A. A. E., 1996, AJ, 111, 414
Gromadzki M., Mikolajewski M., Tomov T., Bellas-Velidis I., Dapergolas A., Galan C., 2006, Acta Astron., 56, 97
Hachisu I., Kato M., Luna G. J. M., 2007, ApJ, 659, 153
Kass R. E., Raftery A. E., 1995, J. Am. Statistical Association, 90, 773

Meyers S., Kelly B., O'Brien J., 1993, Mon. Weather Rev., 121, 2858
Ness J.-U. et al., 2008, ApJ, 665, 1334
Oppenheimer B. D., Mattei J. A., 1993, J. Am. Association Var. Star Obser., 22, 105
Osbourne J. P. et al., 2011, ApJ, 727, 124
Rosino L., 1986, in Bode M. F., ed., RS Ophiuchi (1985) and the Recurrent Nova Phenomenon. VNU Science Press, Utrecht, p. 1
Schaefer B. E., 2004, IAU Circ., 8396
Schwarz G., 1978, Ann. Statistics, 6, 461
Sokoloski J. L., Bildsten L., Ho W. C. G., 2001, MNRAS, 326, 553
Sokoloski J. L., Luna G. J. M., Mukai K., Kenyon S. J., 2006, Nat, 442, 276
Starrfield S., Iliadis C., Hix W. R., 2006, in Bode M. F., Evans A., eds, Classical Novae, 2nd edn. Cambridge Univ. Press, Cambridge, p. 77
Torrence C., Compo G., 1998, Bull. Am. Meteorological Soc., 79, 61
Worters H. L., Eyres S. P. S., Bromage G. E., Osborne J. P., 2007, MNRAS, 379, 1557
Yaron O., Prialnik D., Shara M. M., Kovetz A., 2005, ApJ, 623, 398
Zamanov R. K. et al., 2010, MNRAS, 404, 381

This paper has been typeset from a TEX/LATEX file prepared by the author.

© 2011 The Authors, MNRAS **414,** 2195–2203
Monthly Notices of the Royal Astronomical Society © 2011 RAS